JOC Article
pubs.acs.org/joc

Synthesis, Properties, Crystal Structures, and Semiconductor Characteristics of Naphtho[1,2-*b*:5,6-*b*′]dithiophene and -diselenophene Derivatives

Shoji Shinamura,[†] Eigo Miyazaki,[†] and Kazuo Takimiya*[,†,‡]

[†]*Department of Applied Chemistry, Graduate School of Engineering, Hiroshima University, Higashi-Hiroshima 739-8527, Japan, and* [‡]*Institute for Advanced Materials Research, Hiroshima University, Higashi-Hiroshima 739-8530, Japan*

ktakimi@hiroshima-u.ac.jp

Received December 1, 2009

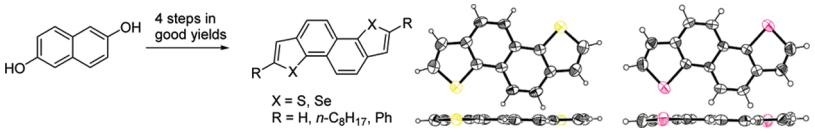

In this paper we present the synthesis, structures, characterization, and applications to field-effect transistors (FETs) of naphtho[1,2-*b*:5,6-*b*′]dithiophene (NDT) and -diselenophene (NDS) derivatives. Treatment of 1,5-dichloro-2,6-diethynylnaphthalenes, easily derived from commercially available 2,6-dihydroxynaphthalene, with sodium chalcogenide afforded a straightforward access to NDTs and NDSs including the parent and dioctyl and diphenyl derivatives. Physicochemical evaluations of NDT and NDS derivatives showed that these heteroarenes have a similar electronic structure with isomeric [1]benzothieno[2,3-*b*][1]benzothiophene (BTBT) and [1]benzoselenopheneno[2,3-*b*][1]benzoselenophene (BSBS) derivatives, respectively. Although attempts to fabricate solution-processed field-effect transistors (FETs) with soluble dioctyl-NDT (C_8-NDT) and -NDS (C_8-NDS) failed, diphenyl derivatives (DPh-NDT and DPh-NDS) afforded vapor-processed FETs showing field-effect mobility as high as 0.7 $cm^2 V^{-1} s^{-1}$. These results indicated that NDT and NDS are new potential heteroarene core structures for organic semiconducting materials.

Introduction

Thiophene-containing fused aromatics, often called heteroarenes, have been important core structures for the development of novel electronic materials.[1] Among numbers of heteroarene systems developed so far, benzodithiophenes (BDTs)[2] and anthradithiophenes (ADTs)[3] have been representatives and used as core structures for organic semiconductors applicable to superior organic field-effect transistors (Figure 1). In sharp contrast, heteroarenes consisting of one naphthalene and two thiophenes in a cata-condensed

(1) (a) Xiao, K.; Liu, Y.; Qi, T.; Zhang, W.; Wang, F.; Gao, J.; Qiu, W.; Ma, Y.; Cui, G.; Chen, S.; Zhan, X.; Yu, G.; Qin, J.; Hu, W.; Zhu, D. *J. Am. Chem. Soc.* **2005**, *127*, 13281–13286. (b) Anthony, J. E. *Chem. Rev.* **2006**, *106*, 5028–5048. (c) Tang, M. L.; Okamoto, T.; Bao, Z. *J. Am. Chem. Soc.* **2006**, *128*, 16002–16003. (d) Yamamoto, T.; Takimiya, K. *J. Am. Chem. Soc.* **2007**, *129*, 2224–2225. (e) Liu, W. J.; Zhou, Y.; Ma, Y.; Cao, Y.; Wang, J.; Pei, J. *Org. Lett.* **2007**, *9*, 4187–4190. (f) Takimiya, K.; Kunugi, Y.; Otsubo, T. *Chem. Lett.* **2007**, *36*, 578–583. (g) Gao, J.; Li, R.; Li, L.; Meng, Q.; Jiang, H.; Li, H.; Hu, W. *Adv. Mater.* **2007**, *19*, 3008–3011. (h) Ebata, H.; Miyazaki, E.; Yamamoto, T.; Takimiya, K. *Org. Lett.* **2007**, *9*, 4499–4502. (i) Gao, P.; Beckmann, D.; Tsao, H. N.; Feng, X.; Enkelmann, V.; Pisula, W.; Müllen, K. *Chem. Commun.* **2008**, 1548–1550. (j) Tang, M. L.; Mannsfeld, S. C. B.; Sun, Y.-S.; Becerril, H. t. A.; Bao, Z. *J. Am. Chem. Soc.* **2009**, *131*, 882–883. (k) Gao, P.; Beckmann, D.; Tsao, H. N.; Feng, X.; Enkelmann, V.; Baumgarten, M.; Pisula, W.; Müllen, K. *Adv. Mater.* **2009**, *21*, 213–216.

(2) (a) Laquindanum, J. G.; Katz, H. E.; Lovinger, A. J.; Dodabalapur, A. *Adv. Mater.* **1997**, *9*, 36–39. (b) Katz, H. E.; Bao, Z.; Gilat, S. L. *Acc. Chem. Res.* **2001**, *34*, 359–369. (c) Takimiya, K.; Kunugi, Y.; Konda, Y.; Niihara, N.; Otsubo, T. *J. Am. Chem. Soc.* **2004**, *126*, 5084–5085. (d) Takimiya, K.; Konda, Y.; Ebata, H.; Niihara, N.; Otsubo, T. *J. Org. Chem.* **2005**, *70*, 10569–10571. (e) Takimiya, K.; Kunugi, Y.; Ebata, H.; Otsubo, T. *Chem. Lett.* **2006**, *35*, 1200–1201. (f) Pan, H.; Li, Y.; Wu, Y.; Liu, P.; Ong, B. S.; Zhu, S.; Xu, G. *Chem. Mater.* **2006**, *18*, 3237–3241. (g) Pan, H.; Li, Y.; Wu, Y.; Liu, P.; Ong, B. S.; Zhu, S.; Xu, G. *J. Am. Chem. Soc.* **2007**, *129*, 4112–4113. (h) Pan, H.; Wu, Y.; Li, Y.; Liu, P.; Ong, B. S.; Zhu, S.; Xu, G. *Adv. Funct. Mater.* **2007**, *17*, 3574–3579. (i) Kashiki, T.; Miyazaki, E.; Takimiya, K. *Chem. Lett.* **2008**, *37*, 284–285. (j) Kashiki, T.; Miyazaki, E.; Takimiya, K. *Chem. Lett.* **2009**, *38*, 568–569. (k) Shinamura, S.; Kashiki, T.; Izawa, T.; Miyazaki, E.; Takimiya, K. *Chem. Lett.* **2009**, *38*, 352–353.

(3) (a) Laquindanum, J. G.; Katz, H. E.; Lovinger, A. J. *J. Am. Chem. Soc.* **1998**, *120*, 664–672. (b) Payne, M. M.; Parkin, S. R.; Anthony, J. E.; Kuo, C. C.; Jackson, T. N. *J. Am. Chem. Soc.* **2005**, *127*, 4986–4987. (c) Shen, H.-C.; Tang, J.-M.; Chang, H.-K.; Yang, C.-W.; Liu, R.-S. *J. Org. Chem.* **2005**, *70*, 10113–10116. (d) Pietrangelo, A.; MacLachlan, M. J.; Wolf, M. O.; Patrick, B. O. *Org. Lett.* **2007**, *9*, 3571–3573. (e) Chen, M.-C.; Kim, C.; Chen, S.-Y.; Chiang, Y.-J.; Chung, M.-C.; Facchetti, A.; Marks, T. J. *J. Mater. Chem.* **2008**, *18*, 1029–1036. (f) Pietrangelo, A.; Patrick, B. O.; MacLachlan, M. J.; Wolf, M. O. *J. Org. Chem.* **2009**, *74*, 4918–4926.

Published on Web 01/25/2010 DOI: 10.1021/jo902545a

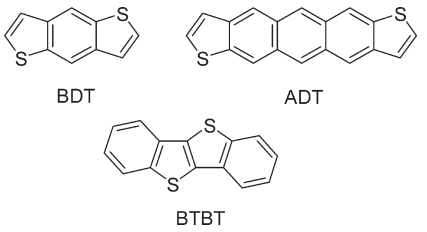

FIGURE 1. Some heteroarene cores for organic semiconductors.

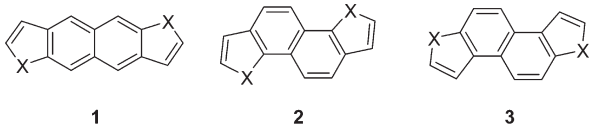

FIGURE 2. C_{2h} symmetrical naphthodichalcogenophene isomers (X = S or Se) as potential organic semiconductor cores.

manner, i.e., naphtodithiophenes (NDTs, Figure 2), have not been examined as organic semiconductors,[4] although several isomeric NDTs have been known[5] and they seem to be promising as core structures for organic semiconductors.[6] This is mainly due to the lack of practical methods for the scalable synthesis of NDTs for further investigation.

We have recently reported a straightforward protocol for thiophene-annulation reactions on a benzene ring to give various benzo[*b*]thiophene derivatives, not only monoannulated ones (benzo[*b*]thiophenes), but also bis-(benzodithiophenes) and tris-annulated derivatives (benzotrithiophenes).[7] One of the merits of this protocol is that one can use easily available *o*-chloro- or *o*-bromo-substituted ethynylbenzenes as a precursor. Taking advantage of the protocol, we examined the syntheses of one of the NDT isomers, naphtho[1,2-*b*:5,6-*b*′]dithiophenes (**2**, Figure 2), and its selenium analogues from 1,5-dichloro-2,6-diethynylnaphthalenes and found that these heteroarenes are easily synthesizable. Since the parent heteroarenes have an isoelectronic structure with [1]benzothieno[2,3-*b*][1]benzothiophene (BTBT, Figure 1)[8] and its selenium analogue (BSBS)[9] that can serve as cores for superior organic semiconductors, it is very interesting to compare the physicochemical properties between NDT/NDS

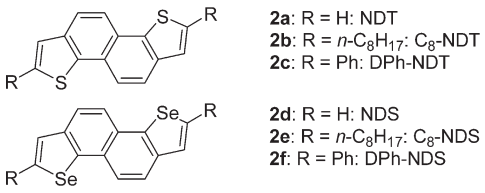

FIGURE 3. Molecular structure of naphtho[1,2-*b*:5,6-*b*′]dithiophenes and -diselenophenes.

SCHEME 1. Synthesis of NDT and NDS Derivatives

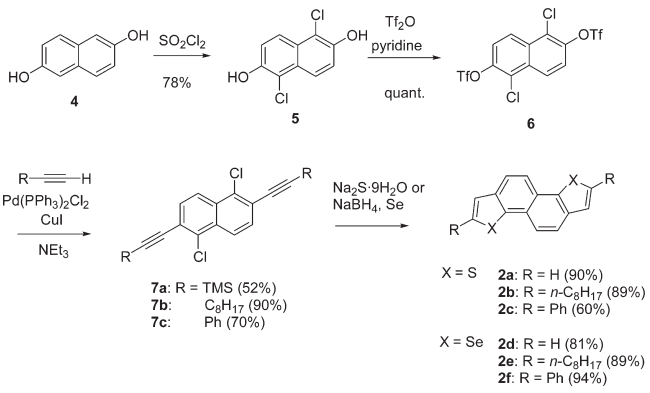

and BTBT/BSBS and to examine NDT and NDS derivatives (Figure 3) as organic semiconducting materials. We here report their synthesis, properties, crystal structure, and semiconductor characteristics.

Results and Discussions

Synthesis. Successful synthetic routes to NDTs and NDSs were shown in Scheme 1. Starting from commercially available 2,6-dihydroxynaphthalene (**4**), selective chlorination at 1- and 5-positions to give **5**[10] followed by a reaction with trifluoromethanesulfonic anhydride gave a key intermediate, 1,5-dichloro-2,6-bis(trifluoromethanesulfonyloxy)naphthalene (**6**). Under the typical Sonogashira coupling conditions, reaction with various terminal acetylenes, e.g., trimethylsilylacetylene, 1-octyne, and phenylacetylene, took place chemoselectively at the triflate sites (2- and 6- positions) on **6** to give the precursors (**7a**−**c**) in moderate to high yields. Final ring-closing reactions that construct fused-thiophene or -selenophene rings were easily accomplished in reasonable yields with sodium chalcogenide reagents as previously reported.[7] All the new materials were fully characterized with spectroscopic analyses and combustion elemental analysis. We also carried out single-crystal X-ray analysis for the parent NDT and NDS, C_8-NDT, and DPh-NDT. All these structural analyses also gave unambiguous identification of the desired compounds in the present synthesis.

Molecular structures of the parent NDT and NDS are depicted in Figure 4a. Both molecules have almost planar structure as expected. In the crystal packing, the molecules of both NDT and NDS form similar layered structures and arrange in herringbone manner in each layer (Figure 4b).

(4) Peri-condensed naphthodithiophene derivatives have been reported: (a) Takimiya, K.; Yashiki, F.; Aso, Y.; Otsubo, T.; Ogura, F. *Chem. Lett.* **1993**, *22*, 365–368. (b) Takimiya, K.; Otsubo, T.; Ogura, F. *J. Chem. Soc., Chem. Commun.* **1994**, 1859–1860. (c) Takimiya, K.; Kato, K.-i.; Aso, Y.; Ogura, F.; Otsubo, T. *Bull. Chem. Soc. Jpn.* **2002**, *75*, 1795–1805. (d) Takimiya, K.; Kunugi, Y.; Toyoshima, Y.; Otsubo, T. *J. Am. Chem. Soc.* **2005**, *127*, 3605–3612.

(5) Synthesis of **2** and **3** (X = S) via flash vacuum pyrolysis (FVP) was recently reported: (a) Umeda, R.; Fukuda, H.; Miki, K.; Rahman, S. M. A.; Sonoda, M.; Tobe, Y. *C. R. Chim.* **2009**, *12*, 378−384. See also: (b) Tilak, B. D. *Proc. Indian Acad. Sci., Sect. A* **1951**, *33A*, 71–77.

(6) Coropceanu, V.; Kwon, O.; Wex, B.; Kaafarani, B. R.; Gruhn, N. E.; Durivage, J. C.; Neckers, D. C.; Bredas, J.-L. *Chem.—Eur. J.* **2006**, *12*, 2073–2080.

(7) Kashiki, T.; Shinamura, S.; Kohara, M.; Miyazaki, E.; Takimiya, K.; Ikeda, M.; Kuwabara, H. *Org. Lett.* **2009**, *11*, 2473–2475.

(8) (a) Takimiya, K.; Ebata, H.; Sakamoto, K.; Izawa, T.; Otsubo, T.; Kunugi, Y. *J. Am. Chem. Soc.* **2006**, *128*, 12604–12605. (b) Ebata, H.; Izawa, T.; Miyazaki, E.; Takimiya, K.; Ikeda, M.; Kuwabara, H.; Yui, T. *J. Am. Chem. Soc.* **2007**, *129*, 15732–15733. (c) Izawa, T.; Miyazaki, E.; Takimiya, K. *Adv. Mater.* **2008**, *20*, 3388–3392. (d) Izawa, T.; Mori, H.; Shinmura, Y.; Iwatani, M.; Miyazaki, E.; Takimiya, K.; Hung, H.-W.; Yahiro, M.; Adachi, C. *Chem. Lett.* **2009**, *38*, 420–421.

(9) (a) Takimiya, K.; Kunugi, Y.; Konda, Y.; Ebata, H.; Toyoshima, Y.; Otsubo, T. *J. Am. Chem. Soc.* **2006**, *128*, 3044–3050. (b) Izawa, T.; Miyazaki, E.; Takimiya, K. *Chem. Mater.* **2009**, *21*, 903–912.

(10) (a) Nakasuji, K.; Sugiura, K.; Kitagawa, T.; Toyoda, J.; Okamoto, H.; Okaniwa, K.; Mitani, T.; Yamamoto, H.; Murata, I. *J. Am. Chem. Soc.* **1991**, *113*, 1862–1864. (b) Willstätter, R.; Parnas, J. *Ber. Dtsch. Chem. Ges.* **1907**, *40*, 3971–3978.

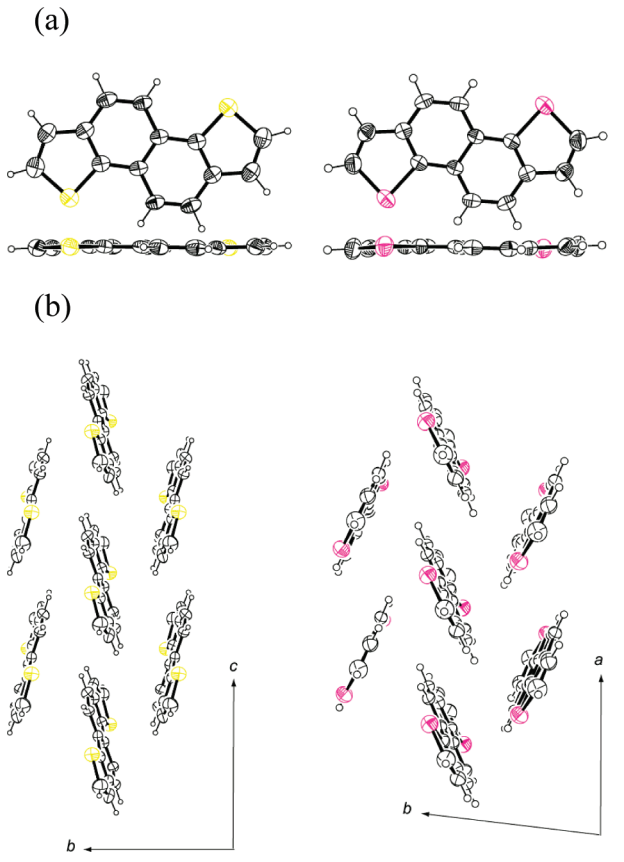

FIGURE 4. Molecular (a) and packing structures (b) of NDT (left) and NDS (right).

Physicochemical Properties. The parent NDT is formally isoelectronic with BTBT and chrysene.[11] Thus, it is interesting to compare the electronic structure of these fused-aromatics to elucidate the structure−property correlations. Figure 5 shows cyclic volatmmograms of NDT, NDS, BTBT, and chrysene, where all four compounds show oxidation peaks in a relatively high potential regime (ca. +1.3−1.5 V vs. Ag/AgCl). Their HOMO energy levels estimated from the onsets of the oxidation peaks are summarized in Table 1.[12] The chalcogenophene-containing compounds tend to have slightly higher HOMO energy levels than chrysene does. In contrast to the quasi-reversible oxidation peak of BTBT, the peaks of NDT and NDS are irreversible without clear reduction processes. In addition, receptive voltammetric scan for the parent NDT and NDS deposited polymer-like film on the working electrode, probably owing to electrochemical homopolymerization at the electrochemically active α-position of thiophene or selenophene at both ends of the molecules (Figure S3, Supporting Information). Although individual features for each compound are observed in the voltammogram, the HOMO energy level is almost the same for the four compounds, reflecting their isoelectronic structures as expected.[11]

Their UV−vis spectra depicted in Figure 6 clearly indicated that all four materials have largely blue-shifted absorptions (up to ca. 350 nm) compared with that of naphthacene (~490 nm, not seen in Figure 6),[11] an acene consisting of four benzene rings, indicating that the electronic structures of NDT and BTBT are rather phene-like. Despite their overall similarity in UV−vis spectra, small differences are observed:

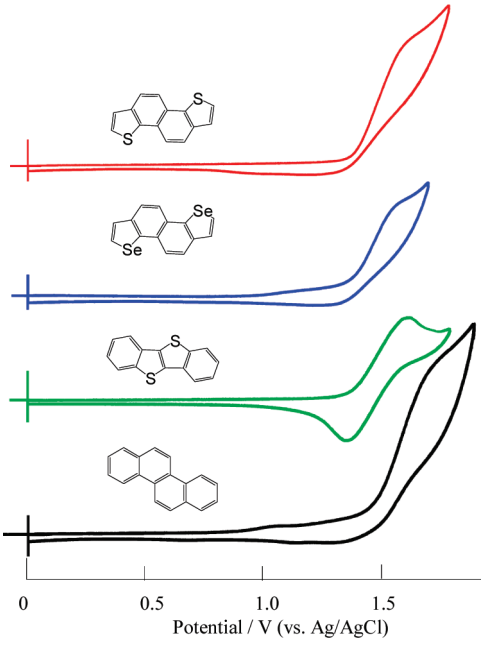

FIGURE 5. Cyclic voltammograms of NDT, NDS, BTBT, and chrysene.

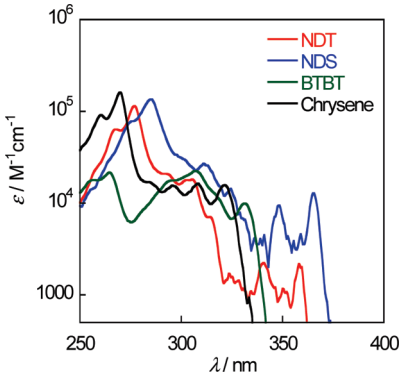

FIGURE 6. UV−vis spectra of NDT, NDS, BTBT, and chrysene in dichloromethane.

TABLE 1. Oxidation Potential, Absorption Edge in UV−Vis Spectra of NDT and NDS Derivatives

compd	E_{onset}/V[a]	HOMO/eV[b]	λ_{edge}/nm	E_g/eV[d]
NDT	1.38	−5.8	320[c]	3.9
NDS	1.36	−5.7	335[c]	3.7
BTBT	1.38	−5.8	340	3.7
chrysene	1.46	−5.9	330	3.8
C_8-NDT	1.25	−5.6	325[c]	3.8
C_8-NDS	1.23	−5.6	340[c]	3.6
DPh-NDT	1.15	−5.5	395	3.1
DPh-NDS	1.18	−5.6	405	3.1

[a] V vs. Ag/AgCl. All the potentials were calibrated with the Fc/Fc^+ ($E^{1/2}$ = +0.43 V measured under identical conditions). [b] Estimated with the following equation: E^{HOMO} (eV) = −4.4 − E_{onset}. [c] Forbidden triplet−triplet bands were not considered. [d] Calculated from λ_{edge}.

(11) Takimiya, K.; Yamamoto, T.; Ebata, H.; Izawa, T. *Sci. Technol. Adv. Mater.* **2007**, *8*, 273–276.
(12) Pommerehne, J.; Vestweber, H.; Guss, W.; Mahrt, R. F.; Bässler, H.; Porsch, M.; Daub, J. *Adv. Mater.* **1995**, *7*, 551–554.

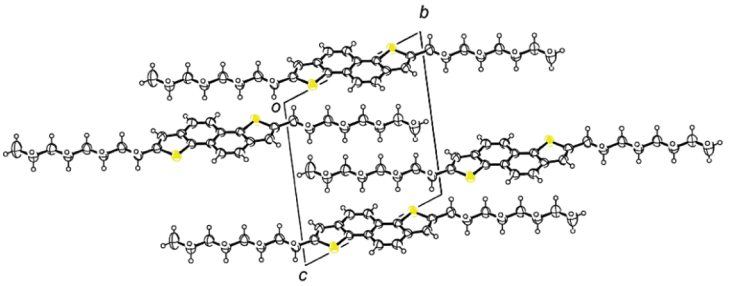

FIGURE 7. Molecular arrangement in a single crystal of C_8-NDT.

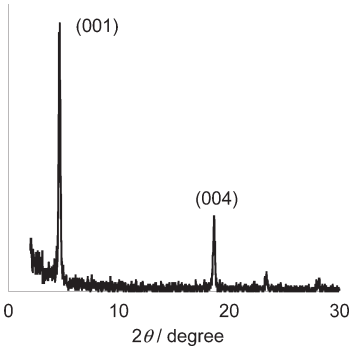

FIGURE 8. XRD pattern of the evaporated thin film of DPh-NDT.

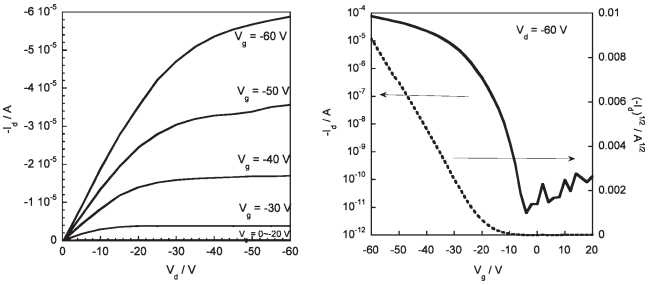

FIGURE 9. Output and transfer characteristics of DPh-NDT-based OFET fabricated on HMDS-treated Si/SiO_2 substrate.

in particular, NDT and NDS have weak, but red-shifted absorption bands up to 360 nm, which reflects marginal difference in their electronic structure. At the present moment, the origin of the red-shifted absorption bands for NDT and NDS is not clear. To help to understand, we carried out time-dependent differential functional theory (TD-DFT) MO calculations[13] for NDT, which suggests that these absorptions can be ascribed to triplet transitions between orbitals near the HOMO-LUMO gaps that are normally forbidden (see the Supporting Information).

Oxidation onsets extracted from CVs and absorption edge from UV−vis spectra of C_8-NDT, DPh-NDT, C_8-NDS, and DPh-NDS were also summarized in Table 1. C_8-NDT and -NDS showed lower oxidation onsets than those of the parent ones, reflecting the electron-donating nature of the alkyl groups. Introduction of phenyl groups not only lowered the oxidation onsets by more than 0.2 V but also caused a large red shift in UV−vis spectra, indicative of extension of π-conjugation. The HOMO energy levels and energy gaps estimated from the oxidation onsets and absorption edges, respectively, for the dialkyl and diphenyl derivatives of NDT and NDS are also similar to those of the corresponding BTBT and BSBS derivatives.[8,9] The similarity in physicochemical properties can be understood by the consideration that the molecular electronic structures of the NDT and NDS derivatives are basically the same as those of the BTBT and BSBS derivatives.

FET Devices. To examine the present NDT and NDS derivatives as organic semiconductors, we fabricated and evaluated their FET devices. Attempts to fabricate FET devices via solution deposition processes using highly soluble C_8-NDT and C_8-NDS unfortunately failed. All the devices showed no filed effect, owing to the poor quality of the films on Si/SiO_2 substrates: only noncontinuous films were deposited and could not cover the channel region of the devices. Besides poor thin film forming properties, the molecular arrangement of C_8-NDT missing effective intermolecular interactions between the NDT cores would not be suitable for effective carrier transport (Figure 7). Thus, it can be concluded that alkylated NDT and NDS are significantly different from their isomeric alkylated BTBTs and BSBSs in terms of film-forming nature and molecular arrangement in the thin film state and the bulk single crystals,[8b,c,9b] although the molecular electronic properties are very similar to each other as discussed above.

In contrast, physical vapor deposition of DPh-NDT and DPh-NDS gave homogeneous thin films on Si/SiO_2 substrates, which also showed crystalline peaks in XRD patterns assignable to layered structure on the substrate (Figure 8). Calculated interlayer spacing for the DPh-NDT thin film (~19 Å) is almost the same as that with the crystallographic *c*-axis of its bulk single crystal and with its molecular length (vide infra).

FET devices with a top contact configuration (W/L = 30) were evaluated under ambient conditions. In the case of DPh-NDT-based devices, devices fabricated at any substrate temperatures (T_{sub}) showed typical p-channel FET responses. The field-effect mobilities extracted from the saturation regime for DPh-NDT-based devices were up to 0.2 $cm^2\ V^{-1}\ s^{-1}$ with a I_{on}/I_{off} ratio of 10^6 (Figure 9). The relatively good device performances of the DPh-NDT-based FETs can be rationalized by the molecular arrangement of DPh-NDT: single-crystal X-ray analysis of DPh-NDT clearly indicated that the DPh-NDT molecules arranged in a herringbone manner (Figure 10), which is an optimal molecular arrangement to give a two-dimensional electronic structure suitable

(13) MO calculations were carried out with the DFT/TD-DFT method at the B3LYP/6-31g(d) level, using the Gaussian 03 program package . Frisch, M. J. et al. *Gaussian 03*, revision C.02; Gaussian, Inc., Wallingford, CT, 2004.

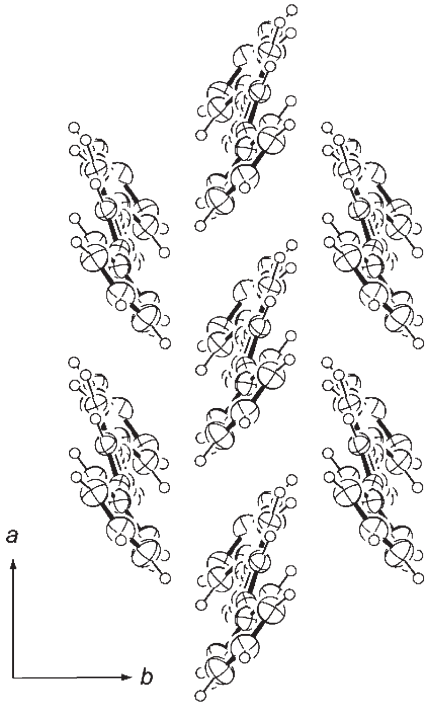

FIGURE 10. Molecular arrangement in a bulk single crystal of DPh-NDT.

TABLE 2. FET Characteristics[a] of DPh-NDT- and DPh-NDS-Based OFETs

compd	T_{sub}[b]/°C	μ_{FET}[c]/cm^2 V^{-1} s^{-1}	I_{on}/I_{off}[d]	V_{th}/V
DPh-NDT	25	0.2	10^5	−19
	60	0.3	10^6	−19
	100	0.3	10^6	−32
DPh-NDS	25	0.7	10^6	−15
	60	0.3	10^6	−30
	100	0.4	10^7	−31

[a] FET devices were fabricated on HMDS-treated substrates with $W/L = 30$. [b] Substrate temperature during vapor deposition of the semiconductors. [c] Extracted from the saturation regime. [d] I_{on} and I_{off} were the source-drain current measured at $V_g = -60$ and 0 V, respectively.

for thin film-based OFETs as was observed for the pentacene thin films.[14] However, compared to the device characteristics of DPh-BTBT, which is isoelectronic with DPh-NDT, the mobility of DPh-NDT-based devices is lower by one order of magnitude than that of the best DPh-BTBT device (μ = 2.0 cm^2 V^{-1} s^{-1}).[8a] At the moment the reasons for the reduced device characteristics are not clear, but we speculate that the extent of intermolecular interaction in the solid state is different between these two compound, since nonbonded sulfur−sulfur contact does not exist in the present DPh-NDT, whereas in general the BTBT-based molecules tend to have effective intermolecular interaction though nonbonded sulfur−sulfur contacts.[8c]

With the selenium analogue, DPh-NDS, the OFETs fabricated under various processing conditions also showed comparable FET characteristics to those of DPh-NDT-based ones, showing μ_{FET} values of up to 0.7 cm^2 V^{-1} s^{-1} (Table 2). Although the exact molecular arrangement in the solid state is not clear, DPh-NDS seems to have a similar packing structure with that of DPh-NDT, since their thin film XRDs with *d*-spacings of ca. 20 Å are similar to each other (Figure S4, Supporting Information). Therefore, we concluded at this moment that the well-ordered molecular array for DPh-NDS similar to that for DPh-NDT also accounted for their relatively high μ_{FET} values. These results indicated that the NDT and NDS frameworks are potential core structures for further development of superior organic semiconductors, provided that suitable molecular modifications for the thin film deposition are made.

Conclusions. In summary, we have successfully established practical syntheses of naphtho[1,2-*b*:5,6-*b*′]dithiophene (NDT) and -diselenophene (NDS) derivatives, taking advantage of the thiophene- and selenophene-annulation protocol recently developed in our group. Physicochemical evaluation of the NDT and NDS derivatives indicated that they are isostructural with corresponding BTBT and BSBS derivatives, respectively. Through the present screening research of the NDT and NDS derivatives as organic semiconductors for OFET devices, we found that the dipheneyl derivatives, DPh-NDT and DPh-NDS, are promising materials for high-performance organic semiconductors with relatively high mobility up to 0.7 cm^2 V^{-1} s^{-1}. These results indicate that NDT and NDS are potential cores for the development of organic semiconductors similar to their isoelectronic heteroarens, BTBT and BSBS. Different from BTBT and BSBS, an interesting feature of the NDT/NDS system is that they have vacant α positions of thiophene or selenophene rings, at which various chemical or electrochemical reactions can take place easily and selectively. Thus, NDT and NDS will be useful cores not only for small molecule-based organic semiconductors but also polymer semiconductors. Further investigations to develop new materials via chemical modifications are now actively being conducted in our research group.

Experimental Section

Synthesis: General. All chemicals and solvents are of reagent grade unless otherwise indicated. Triethylamine, ethanol, tetrahydrofuran (THF), and *N*-methyl-2-pyrrolidone (NMP) were purified with standard distillation procedures prior to use. All reactions were carried out under nitrogen atmosphere. Melting points were uncorrected. Nuclear magnetic resonance spectra were obtained in deuterated chloroform with TMS as internal reference; chemical shifts (δ) are reported in parts per million. EI-MS spectra were obtained with use of an electron impact ionization procedure (70 eV). The molecular ion peaks of the chlorine-, sulfur-, or selenium-containing compounds showed a typical isotopic pattern, and all the mass peaks are reported based on ^{35}Cl, ^{32}S, or ^{80}Se, respectively.

1,5-Dichloro-2,6-dihydroxynaphthalene (5)[10]. To a solution of 2,6-dihydroxynaphthalene (**4**, 3.0 g, 18.7 mmol) in glacial acetic acid (90 mL) was slowly added sulfuryl chloride (3.0 mL, 37.5 mmol) at 0 °C. After the mixture was stirred for 5 h, water (50 mL) was added, and the resulting precipitate was collected by filtration and washed with water to give 1,5-dichloro-2,6-dihydroxynaphthalene as a white solid (3.3 g, 78%). Mp 230.0−230.5 °C (lit.[10] mp 223.5 °C); ^{1}H NMR δ 5.79 (s, 2H), 7.35 (d, J = 8.9 Hz, 2H), 7.96 (d, J = 8.9 Hz, 2H); EIMS m/z 228 (M^+).

1,5-Dichloro-2,6-bis(trifluoromethanesulfonyloxy)naphthalene (6). To a suspension of 1,5-dichloro-2,6-dihydroxynaphthalene (**5**, 2.3 g, 10 mmol) and pyridine (4.8 mL, 60 mmol) in dichloromethane (100 mL) was slowly added trifluoromethanesulfonic anhydride (3.6 mL, 22 mmol) at 0 °C. After the mixture was stirred for 18 h, water (10 mL) and hydrochloric acid (1 M, 10 mL) were

(14) Cornil, J.; Calbert, J. P.; Bredas, J. L. *J. Am. Chem. Soc.* **2001**, *123*, 1250–1251.

added. The resulting mixture was extracted with dichloromethane (3 × 20 mL), and the combined organic layer was dried ($MgSO_4$) and concentrated in vacuo. The residue was purified by column chromatography on silica gel eluted with dichloromethane (R_f 0.95) to give 1,5-dichloro-2,6-bis(trifluoromethanesulfonyloxy)-naphthalene as a white solid (4.9 g, 99%). ^{1}H NMR δ 7.68 (d, J = 9.3 Hz, 2H), 8.40 (d, J = 9.3 Hz, 2H); ^{13}C NMR δ 118.8 (q, $^2J_{C-F}$ = 322.5 Hz), 122.9, 125.6, 126.2, 131.4, 144.9; EIMS m/z 492 (M^+); mp 127.2−128.0 °C. Anal. Calcd for $C_{12}H_4Cl_2F_6O_6S_2$: C, 29.22; H, 0.82. Found: C, 29.44; H, 0.76.

General Procedure for the Palladium-Catalyzed Sonogashira Coupling of 1,5-Dichloro-2,6-bis(trifluoromethanesulfonyloxy)-naphthalene (6) with Terminal Alkynes. To a deaerated solution of 1,5-dichloro-2,6-bis(trifluoromethanesulfonyloxy)naphthalene (**6**, 493 mg, 1.0 mmol) and triethylamine (0.42 mL, 3.0 mmol) in THF (10 mL) were added $Pd(PPh_3)_2Cl_2$ (70 mg, 0.05 mmol, 10 mol %), CuI (38 mg, 0.1 mmol, 20 mol %), and terminal alkyne (3.0 mmol). After the mixture was refluxed for 20 h, water (1 mL) and hydrochloric acid (1 M, 1 mL) were added. The resulting mixture was extracted with dichloromethane (3 × 5 mL), and the combined organic layer was dried ($MgSO_4$) and concentrated in vacuo. The residue was purified by column chromatography on silica gel eluted with hexane to give 1,5-dichloro-2,6-dietynylnaphthalene analogue (**7**) as a white solid.

1,5-Dichloro-2,6-bis(trimethylsilylethynyl)naphthalene (7a): 52% yield; Mp 217.0−218.0 °C; ^{1}H NMR δ 0.31 (s, 18H), 7.61 (d, J = 8.8 Hz, 2H), 8.12 (d, J = 8.8 Hz, 2H); ^{13}C NMR δ 0.1, 101.8, 103.0, 122.0, 123.7, 130.7, 131.3, 134.8; EIMS m/z 388 (M^+). Anal. Calcd for $C_{20}H_{22}Cl_2Si_2$: C, 61.68; H, 5.69. Found: C, 61.45; H, 5.51.

1,5-Dichloro-2,6-di(decyn-1-yl)naphthalene (7b): 90% yield; Mp 44.0−44.5 °C; ^{1}H NMR δ 0.89 (t, J = 7.0 Hz, 6H), 1.23−1.71 (m, 24H), 2.53 (t, J = 7.0 Hz, 4H), 7.56 (d, J = 8.5 Hz, 2H), 8.13 (d, J = 8.5 Hz, 2H); ^{13}C NMR δ 14.2, 19.9, 22.8, 28.7, 29.0, 29.2, 29.3, 32.0, 78.5, 98.6, 122.5, 123.5, 130.7, 131.0, 133.8; EIMS m/z 468 (M^+). Anal. Calcd for $C_{30}H_{38}Cl_2$: C, 76.74; H, 8.16. Found: C, 76.74; H, 8.31.

1,5-Dichloro-2,6-bis(phenylethynyl)naphthalene (7c): 70% yield; Mp 200.5−201.0 °C; ^{1}H NMR δ 7.39−7.42 (m, 6H), 7.63−7.67 (m, 4H), 7.74 (d, J = 8.6 Hz, 2H), 8.25 (d, J = 8.6 Hz, 2H); EIMS m/z 396 (M^+). Anal. Calcd for $C_{26}H_{14}Cl_2$: C, 78.60; H, 3.55. Found: C, 78.39; H, 3.34.

Naphtho[1,2-*b*:5,6-*b*′]dithiophene (NDT, 2a). A suspension of $Na_2S\cdot 9H_2O$ (615 mg, 2.56 mmol) in NMP (15 mL) was stirred for 15 min at room temperature. To the mixture was added 1,5-dichloro-2,6-bis(trimethylsilylethynyl)naphthalene (**7a**, 250 mg, 0.64 mmol), and the resulting mixture was heated at 185 °C for 12 h. After cooling, the mixture was poured into saturated aqueous ammonium chloride solution (50 mL). The resulting precipitate was collected by filtration and purified by column chromatography on silica gel eluted with hexane (R_f 0.2) to give naphtho[1,2-*b*:5,6-*b*′]dithiophene (NDT, 139 mg, 90%) as a white solid. Mp 150.4−150.8 °C; ^{1}H NMR δ 7.50 (d, J = 5.3 Hz, 2H), 7.54 (d, J = 5.3 Hz, 2H), 7.95 (d, J = 8.6 Hz, 2H), 8.07 (d, J = 8.6 Hz, 2H); ^{13}C NMR δ 121.3, 122.8, 125.3, 125.4, 126.2, 137.4, 138.6; EIMS m/z 240 (M^+). Anal. Calcd for $C_{14}H_8S_2$: C, 69.96; H, 3.35. Found: C, 69.95; H, 3.26.

2,7-Dioctylnaphtho[1,2-*b*:5,6-*b*′]dithiophene (C_8-NDT, 2b). A similar procedure as above with use of 1,5-dichloro-2,6-di(decyn-1-yl)naphthalene (**7b**) gave the title compound in 89% yield. Mp 92.0−93.0 °C; ^{1}H NMR δ 0.88 (t, J = 6.8 Hz, 6H), 1.21−1.83 (m, 24H), 2.97 (t, J = 7.4 Hz, 4H), 7.14 (s, 2H), 7.77 (d, J = 8.6 Hz, 2H), 7.91 (d, J = 8.6 Hz, 2H); ^{13}C NMR δ 14.2, 22.8, 29.3, 29.4, 29.5, 30.9, 31.5, 32.0, 120.9, 122.0, 122.1, 125.7, 137.4, 137.6, 145.8; EIMS m/z 464 (M^+). Anal. Calcd for $C_{30}H_{40}S_2$: C, 77.53; H, 8.67. Found: C, 77.46; H, 8.71.

2,7-Diphenylnaphtho[1,2-*b*:5,6-*b*′]dithiophene (DPh-NDT, 2c). A suspension of $Na_2S\cdot 9H_2O$ (608 mg, 2.53 mmol) in NMP (15 mL) was stirred for 15 min at room temperature. To the mixture was added 1,5-dichloro-2,6-bis(phenylethynyl)naphthalene (**7c**, 250 mg, 0.63 mmol), and the resulting mixture was heated at 185 °C for 12 h. After cooling, the mixture was poured into saturated aqueous ammonium chloride solution (50 mL). The resulting precipitate was collected by filtration and washed with water. The crude solid was purified by vacuum sublimation to give analytical 2,7-diphenylnaphtho[1,2-*b*:5,6-*b*′]dithiophene (147 mg, 60%) as a pale yellow solid. Mp >300 °C; ^{1}H NMR δ 7.34−7.40 (m, 2H), 7.45−7.57 (m, 4H), 7.71 (s, 2H), 7.79−7.82 (m, 4H), 7.91 (d, J = 8.6 Hz, 2H), 8.05 (d, J = 8.6 Hz, 2H); ^{13}C NMR δ 121.4, 122.8, 125.3, 125.4, 126.2, 137.4, 138.6; EIMS m/z 392 (M^+). Anal. Calcd for $C_{26}H_{16}S_2$: C, 79.55; H, 4.11. Found: C, 79.31; H, 3.81.

Naphtho[1,2-*b*:5,6-*b*′]diselenophene (NDS, 2d). To a suspension of selenium powder (72 mg, 0.91 mmol) in ethanol (3 mL) was added sodium borohydride ($NaBH_4$, 34 mg, 0.91 mmol) at ice-bath temperature. After the mixture was stirred for 40 min at the same temperature, NMP (10 mL) and 1,5-dichloro-2,6-bis(trimethylsilylethynyl)naphthalene (**7a**, 100 mg, 0.26 mmol) were added. The mixture was heated at 185 °C with distilling out ethanol with use of a Dean−Stark condenser for 12 h. After cooling, the mixture was poured into saturated aqueous ammonium chloride solution (50 mL). The resulting precipitate was collected by filtration and purified by column chromatography on silica gel eluted with hexane (R_f 0.2) to give naphtho[1,2-*b*:5,6-*b*′]diselenophene (70 mg, 81%) as a white solid. Mp 193.0−193.5 °C; ^{1}H NMR δ 7.73 (d, J = 5.8 Hz, 2H), 7.92 (s, 4H), 8.08 (d, J = 5.86 Hz, 2H); ^{13}C NMR δ 123.6, 124.4, 128.4, 128.4, 129.2, 140.0, 142.2; EIMS m/z 336 (M^+). Anal. Calcd for $C_{14}H_8Se_2$: C, 50.32; H, 2.41. Found: C, 50.34; H, 2.14.

2,7-Dioctylnaphtho[1,2-*b*:5,6-*b*′]diselenophene (C_8-NDS, 2e). A similar procedure as above with 1,5-dichloro-2,6-di(decyn-1-yl)naphthalene (**7b**) gave the title compound in 89% yield. Mp 130.5−131.0 °C; ^{1}H NMR δ 7.73 (d, J = 5.8 Hz, 2H), 7.92 (s, 4H), 8.08 (d, J = 5.86 Hz, 2H); ^{13}C NMR δ 14.2, 22.8, 29.2, 29.3, 29.5, 32.0, 32.3, 33.4, 123.1, 123.7, 125.5, 128.0, 139.9, 141.1, 151.0; EIMS m/z 560 (M^+). Anal. Calcd for $C_{30}H_{40}Se_2$: C, 64.51; H, 7.22. Found: C, 64.56; H, 7.27.

2,7-Diphenylnaphtho[1,2-*b*:5,6-*b*′]dithiophene (DPh-NDS, 2f). To a suspension of selenium powder (141 mg, 1.8 mmol) in ethanol (4 mL) was added sodium borohydride (68 mg, 1.8 mmol) at ice-bath temperature. After the mixture was stirred for 40 min at the same temperature, NMP (20 mL) and 1,5-dichloro-2,6-bis(phenylethynyl)naphthalene (**7c**, 200 mg, 0.5 mmol) were added. Then, the mixture was heated at 185 °C with distilling out ethanol with use of a Dean−Stark trap for 12 h. After cooling, the resulting mixture was added into saturated aqueous ammonium chloride solution (50 mL). The resulting precipitate was collected by filtration, washed with water, and dried. Continuous extraction from the solid with boiling chloroform afforded 2,7-diphenylnaphtho[1,2-*b*:5,6-*b*′]dithiophene as a pale yellow solid (230 mg, 94%). For device fabrication, DPh-NDS was further purified by vacuum sublimation. Mp >300 °C; EIMS m/z 488 (M^+). Anal. Calcd for $C_{26}H_{16}Se_2$: C, 64.21; H, 3.32. Found: C, 63.84; H, 3.16.

X-ray Crystallographic Analysis. Recrystallization from appropriate solvents for respective compounds gave single crystals suitable for X-ray crystallographic analysis: NDT (hexane), NDS, (hexane), C_8-NDT (chloroform), and DPh-NDT (NMP). The X-ray crystal structure analysis was made on a Rigaku RAPID-IP (Mo Kα radiation, λ = 0.71069 Å, graphite monochromator, T = 296 K, ω scan, $2\theta_{max}$ = 55.0°) or on a Rigaku Mercury-CCD (Mo Kα radiation, λ = 0.71069 Å, graphite monochromator, T = 296 K, $2\theta_{max}$ = 55.0°). The structure was solved by the direct methods.[15] Non-hydrogen atoms were refined anisotropically, and hydrogen atoms were included in the calculations but not

(15) SHELXL (SHELX97): Schldric, G. M. Programs for the refinement of crystal structures; University of Goettingen, Goettingen, Germany, 1997.

refined. All calculations were performed with the crystallographic software package TeXsan 1.2.[16] Crystallographic data are summarized in Table S1 (Supporting Information).

Device Fabrication. Si/SiO_2 substrates were exposed to HMDS (hexamethyldisilazane) vapor at room temperature in a closed desiccator under nitrogen overnight.[17] OFETs were fabricated in a "top-contact" configuration on a heavily doped n^+-Si (100) wafer with a 200 nm thermally grown SiO_2 (C_i = 17.3 nF cm^{-2}). A thin film (50 nm thick) of DPh-NDT or DPh-NDS as an active layer was vacuum-deposited on the Si/SiO_2 substrate maintained at various temperatures (T_{sub}) at a deposition rate of ca. 1 Å s^{-1} under a pressure of $\sim 10^{-3}$ Pa. On top of the organic thin film, gold films (80 nm) as drain and source electrodes were deposited through a shadow mask. For a typical device, the drain−source channel length (L) and width (W) are 50 μm and 1.5 mm, respectively. Characteristics of the OFET devices were measured at room temperature under vacuum or in the air with a Keithley 4200 semiconducting parameter analyzer. Field-effect mobility (μ_{FET}) was calculated in the saturation regime (V_d = −60 V) of the I_d, using the following equation:

$$I_d = (WC_i/2L)\mu_{FET}(V_g - V_{th})^2$$

where C_i is the capacitance of the SiO_2 insulator, and V_g and V_{th} are the gate and threshold voltages, respectively. The current on/off ratio (I_{on}/I_{off}) was determined from the I_d at V_g = 0 (I_{off}) and −60 V (I_{on}). The μ_{FET} data reported in Table 2 are typical values from more than five different devices.

(16) *teXsan: Single Crystal Structure Analysis Software*, Version 1.19; Molecular Structure Corporation and Rigaku Corporation, **2000**.

(17) Yoon, M.-H.; DiBenedetto, S. A.; Facchetti, A.; Marks, T. J. *J. Am. Chem. Soc.* **2005**, *127*, 1348–1349.

Physicochemical Studies. UV−vis spectra were measured in dichloromethane or THF solution (concentration: 10^{-5}−10^{-6} M). Cyclic voltammograms (CVs) were recorded on a Hokuto Denko HA-301 potentiostat and a Hokuto Denko HB-104 function generator in benzonitrile containing tetrabutylammonium hexafluorophosphate (Bu_4NPF_6, 0.1 M) as supporting electrolyte at a scan rate of 100 mV/s. Counter and working electrodes were made of Pt, and the reference electrode was Ag/AgCl. All the potentials were calibrated with the standard ferrocene/ferrocenium redox couple (Fc/Fc^+: $E^{1/2}$ = +0.43 V measured under identical conditions). X-ray diffractions of thin films deposited on the Si/SiO_2 substrate were obtained with a Rigaku Ultima IV diffractometer with a Cu Kα source (λ = 1.541 Å) in the air. AFM images of thin films on Si/SiO_2 were obtained by using a Molecular Imaging PicoPlus microscope in air.

Acknowledgment. This work was partially supported by a Grant-in-Aid for Scientific Research (No. 20350088) from the Ministry of Education, Culture, Sports, Science and Technology, Japan.

Supporting Information Available: ^{1}H and ^{13}C NMR spectra of reported compounds including the intermediates, crystallographic information files (CIFs) for NDT, NDS, C_8-NDT, and DPh-NDT, complete ref 13, results on MO calculations, XRD patterns, and AFM images of evaporated thin films of DPh-NDT and DPh-NDS, and output and transfer characteristics of DPh-NDS-based OFETs. This material is available free of charge via the Internet at http://pubs.acs.org.